Journal of Environmental Chemical Engineering 11 (2023) 109454

Contents lists available at ScienceDirect

Journal of Environmental Chemical Engineering

journal homepage: www.elsevier.com/locate/jece

A semi-industrial AnMBR plant for urban wastewater treatment at ambient temperature: Analysis of the filtration process, energy balance and quantification of GHG emissions

A. Jiménez-Benítez [a,*], A. Ruiz-Martínez [a], Á. Robles [a], J. Serralta [b], J. Ribes [a], F. Rogalla [c], A. Seco [a], J. Ferrer [b]

[a] CALAGUA – Unidad Mixta UV-UPV, Departament d'Enginyeria Química, Universitat de València, Avinguda de la Universitat s/n, 46100 Burjassot, Valencia, Spain
[b] CALAGUA – Unidad Mixta UV-UPV, Institut Universitari d'Investigació d'Enginyeria de l'Aigua i Medi Ambient – IIAMA, Universitat Politècnica de Valencia, Camí de Vera s/n, 46022 Valencia, Spain
[c] FCC Aqualia, S.A., Avenida Camino de Santiago, 40, 28050 Madrid, Spain

ARTICLE INFO

Editor: Chao He

Keywords:
Anaerobic membrane bioreactor
Ultrafiltration process
Demonstration plant
Energy balance
Greenhouse gas emissions

ABSTRACT

A semi-industrial scale AnMBR urban wastewater treatment plant was operated for 580 days at ambient temperature (ranging from 10 to 30 °C) to assess its long-term filtration performance, energy balance and GHG emissions. The applied 20ºC-standardized transmembrane flux (J_{20}) was varied between 15 and 25 LMH and the specific gas demand per m^2 of membrane (SGD_m) was modified between 0.10 and 0.40 $Nm^3 \cdot m^{-2} \cdot h^{-1}$ (corresponding to a specific gas demand per permeate volume (SGD_P) between 10 and 20 $Nm^3 \cdot m^{-3}$). The filtration strategy allowed successful long-term operations without any chemical cleaning requirements and little fouling for 233 days. The plant operated as a net energy producer for more than 50 % of the experimental period, with an average net energy demand of − 0.169 ± 0.341, − 0.190 ± 0.376 and − 0.205 ± 0.447 $kWh \cdot m^{-3}$, considering 0 %, 50 % and 70 % of dissolved methane recovery, respectively. Finally, demethanization of AnMBR effluent is needed to achieve an environmentally sustainable operation of the technology. Therefore, the combination of AnMBR with degassing membranes appears as a suitable alternative to conventional wastewater treatment.

1. Introduction

Although conventional wastewater treatment is usually based on aerobic processes (with conventional activated sludge (CAS) or an aerobic membrane bioreactor (MBR)), anaerobic membrane bioreactors (AnMBRs) are receiving increasing attention due to their advantages [1] including: i) organic matter valorization through methane production during anaerobic digestion; ii) a high-quality solid-free effluent production; iii) nutrients are conserved for recovery from the effluent; iv) operations at high sludge retention time (SRT), since membranes decouple hydraulic retention time (HRT) and SRT; v) they can treat low-loaded streams at ambient temperature since the membranes guarantee solids retention and avoid biomass washout; vi) improved stabilization of biosolids and significant reduction in sludge production when long SRTs are applied; and vii) they make reduced layouts possible thanks to the settlers being substituted for compact membrane units.

AnMBR technology has been considered for the treatment of different industrial wastewater streams, such as textile, petrochemical, brewing or pharmaceutical industry effluents with satisfactory results [13,5]. However, despite the potential benefits of AnMBR plants for treating urban wastewater (UWW), they still face bottlenecks that need to be overcome, including: i) membrane fouling; ii) eutrophication potential of the effluent when it is discharged in sensitive zones; iii) dissolved methane in the effluent [39]; and iv) competition between sulfate-reducing bacteria (SRB) and methanogens, which can affect methane yield and generate corrosive sulfide [7].

Abbreviations: AnMBR, anaerobic membrane bioreactor; BOD_5, biological oxygen demand; CAS, conventional activated sludge; COD, chemical oxygen demand; GHG, greenhouse gas; HRT, hydraulic retention time; J_{20}, 20ºC-standardized transmembrane flux; N, nitrogen; MBR, membrane bioreactor; P, phosphorus; SGD_m, sparging gas demand per m^2 of membrane; SGD_P, sparging gas demand per m^3 of permeate; SRB, sulfate-reducing bacteria; SRT, sludge retention time; TSS, total suspended solids; UWW, urban wastewater; VSS, volatile suspended solids.

* Corresponding author.
E-mail address: antonio.jimenez@uv.es (A. Jiménez-Benítez).

https://doi.org/10.1016/j.jece.2023.109454
Received 17 November 2022; Received in revised form 25 January 2023; Accepted 5 February 2023
Available online 7 February 2023

Membrane fouling has been extensively identified as a key issue to be addressed before AnMBRs can be widely used for UWW [19]. This phenomenon is governed by different interrelated factors. For instance, operating at high temperatures reduces the viscosity of the mixed liquor, which favors filtration but also involves the release of extracellular polymeric substances (EPS), which are related to fouling [21]. Although anti-fouling strategies based on gas sparging have been reported as effective, they increase the filtration energy demand and introduce shear forces. Increased SRT can also reduce membrane fouling since it consumes EPS and SMP. However, high SRT increases the solids concentration and hinders the progress of filtration.

The loss of part of the methane production as gas dissolved in the effluent must also be addressed to reduce fugitive emissions, identified as one of the greatest contributions to GHG of this technology [38], and to improve the energy performance of the facilities by recovering part of the methane produced [41]. Among other technologies, degasification membranes [35] and spray aeration towers are thus being studied for this aim.

AnMBR plants have been reported to have a lower energy consumption than CAS and MBR; Lazarova et al. [20] reported energy demands of 0.25–0.60 $kWh{\cdot}m^{-3}$ for CAS and 0.50–2.50 $kWh{\cdot}m^{-3}$ for MBR. Pretel et al. [25] reported AnMBR net energy production of 0.17–0.19 $kWh{\cdot}m^{-3}$ without considering dissolved methane recovery, while Jiménez-Benítez et al. [16] reported net energy production of up to 0.47 $kWh{\cdot}m^{-3}$ when treating high-loaded UWW at mild temperatures when dissolved methane was considered and sulfate content in the influent was 112–172 mg $S\text{-}SO_4{\cdot}L^{-1}$. The recovery of organic matter through biogas production makes it possible to partially offset the indirect GHG emissions derived from its energy demand. Also, anaerobic processes do not emit nitrous oxide (N_2O), as do aerobic nitrification/denitrification processes [32]. This is an important feature since the global warming potential of this gas has been estimated at 298 $kgCO_{2eq}$ per kg of N_2O [34].

For all the above reasons, AnMBRs appear as a promising technology for the so-called *water resource recovery facility* concept [10], as opposed to the conventional urban wastewater treatment approach, which considers wastewater as a source of pollution.

This paper evaluates the performance of a semi-industrial AnMBR plant in terms of filtration process performance, energy balance and GHG emissions. The plant was fed with effluent from the pre-treatment of the "Alcázar de San Juan" wastewater treatment plant (Ciudad Real, Spain). The major novelties of this study include i) long-term operation of 580 days; and ii) technical characteristics and operation (real UWW, reactor volume of volume 40 m^3, commercial hollow-fiber membranes, industrial equipment, ambient conditions, etc.). These characteristics allowed obtaining robust data for scaling-up AnMBR technology to full-scale facilities, thus providing of useful information in terms of membrane performance, energy balance, and GHG emissions for the design and full-scale operation of AnMBR systems. The goal of the research was to determine the potential of AnMBR over conventional treatments by assessing its robustness against variations in the main operating conditions (temperature, organic load, treatment flow, etc).

2. Materials and methods

2.1. AnMBR description

The semi-industrial AnMBR plant implemented in the study consisted mainly of the following components: an anaerobic reactor (40-m^3 total volume; 34.4-m^3 working volume); three membrane tanks (MT_A, MT_B and MT_C; 0.8-m^3 total volume each; 0.7-m^3 working volume each) equipped with an ultrafiltration membrane system (PURON® PSH41, KMS, 0.03-μm pore size, 41-m^2 filtration area per tank); a sieve screw (1.5-mm screen size); an equalization tank (1.1 m^3); and a clean-in-place (CIP) tank (0.37 m^3). By including three identical MTs in the system, the effect of applying different J_{20} and gas-assisted membrane scouring intensities on membrane fouling can be tested in parallel treating the same feed at the same ambient conditions. Further details of this system can be found elsewhere in [31] and in supplementary materials. The plant was also equipped with a degassing membrane unit (2.1-m^2 filtration area) for dissolved methane recovery (PermSelect®, MedArray Inc. USA), using vacuum pressure as the driving force (for further details see Sanchis-Perucho et al. [36]).

The AnMBR was fed with effluent from the pre-treatment of the "Alcázar de San Juan" wastewater treatment plant (Ciudad Real, Spain), consisting of screening, grit and grease removal. The average influent quality is shown in Table 1. Since the dairy and wine industries are important elements in the local economy, the influent wastewater was characterized by high concentrations of COD (1071 ± 467 $mg{\cdot}L^{-1}$), BOD_5 (710 ± 274 $mg{\cdot}L^{-1}$) and sulfate (140.3 ± 42.5 mg $SO_4\text{-}S{\cdot}L^{-1}$).

2.2. AnMBR operation

The evolution of HRT, temperature, and organic load available for methanogenesis (OL-MA) during the 580-days experimental operation can be found elsewhere in Robles et al. [29] and in supplementary materials. Temperature varied freely in the 10–30 °C range according to ambient conditions and season and SRT was set to 70 d. Several periods with different average HRT were operated as follows: 40 h (days 1–32); 25 h (days 33–122); 46 h (days 123–170); 38 h (days 171–291); 26 h (day 292–500) and 70 h (days 501–580). The different HRT simulated population changes during the summer and winter periods. Eventually, HRT was stablished at 70 h in a final experimental stage in order to assess the treatment process performance at high HRT.

The number of membrane tanks in operation depended on the selected HRT, while OL-MA was affected by economic activity, mainly dairy and wine, the latter with a markedly seasonal contribution. The influence of the grape harvest and winemaking can be noted between August and October between days 60 (August) and 100 (October) and between days 430 (September) and 480 (October).

Membrane filtration and scouring took place within the following parameter range: the gross 20ºC-standardized transmembrane flux (J_{20}) was modified between 15 and 25 LMH and the specific gas demand per m^2 of membrane (SGD_m) was between 0.10 and 0.40 $Nm^3{\cdot}m^{-2}{\cdot}h^{-1}$, resulting in a specific gas demand per permeate volume (SGD_P) of between 10 and 20 $Nm^3{\cdot}m^{-3}$, (for further details of membrane operation see Robles et al. [30]).

Membranes were operated according to a specific schedule involving a combination of different individual stages taken from a basic 300 s-filtration: 30 s-relaxation cycle. Besides classical membrane operating stages (filtration, relaxation, and back-flush), degasification and ventilation stages were also considered in the membrane operation. Degasification aims to recover the accumulated biogas in top of the dead-end, hollow-fiber membranes, since this accumulation of biogas reduces the effective filtration area. The degasification stage consists of a period of high flow-rate filtration that is carried out to enhance the filtration process efficiency by removing the accumulated biogas. On the other hand, during ventilation, permeate is pumped from the CIP tank to the membrane tank through the degasification vessel instead of through the membrane. The aim of the ventilation stage is to recover the accumulated biogas in the degasification vessel due to the extraction of gas

Table 1
Average influent wastewater characteristics.

Parameter	*Unit*	*Mean ± SD*
TSS	$mg\ TSS{\cdot}L^{-1}$	405 ± 215
Total COD	$mg\ COD{\cdot}L^{-1}$	1071 ± 467
BOD_5	$mg\ COD{\cdot}L^{-1}$	710 ± 274
Total Nitrogen	$mg\ N{\cdot}L^{-1}$	48.2 ± 11.7
Total Phosphorus	$mg\ P{\cdot}L^{-1}$	8.4 ± 2.4
Sulfate	$mg\ SO_4\text{-}S{\cdot}L^{-1}$	140.3 ± 42.5

bubbles during filtration.

The chemical membrane cleaning included a first washing phase with sodium hypochlorite (2000 ppm) for 8 h followed by a second washing phase with citric acid (2000 ppm) for another 8 h.

The size of the AnMBR plant and the type and quality of the wastewater (real urban wastewater) involved in this study can contribute to determine the conditions for the technical, economic and environmental feasibility of these technologies as an alternative to conventional wastewater treatment.

2.3. Streams characterization and analytical methods

The following parameters were regularly monitored in the influent: total chemical oxygen demand (COD), biological oxygen demand (BOD_5), sulfate, sulfide, total suspended solids (TSS), and volatile suspended solids (VSS). Effluent quality was mainly monitored through COD, sulfide and volatile fatty acids content. Reactor monitoring was based on TSS, VSS, COD, pH and methane content in the generated biogas (% CH_4). TSS, VSS, COD, BOD_5, sulfate and sulfide were determined according to standard methods [2]. VFA concentration was determined by titration according to the method proposed by [27]). Dissolved methane in the effluent was determined according to Giménez et al. [9].

2.4. Data processing and calculations

The instrumentation implemented in the prototype acquired the following data, among others: reactor influent flow, reactor temperature, transmembrane pressures and fluxes, biogas flows for reactor mixing and membrane scouring, mixed liquor feeding flow to the membrane tanks, and biogas production and quality. Different key performance indicators were calculated to assess the performance of the system, i.e. J_{20}, specific energy consumption (EC), total energy recovery (TER), net energy demand (NED) and greenhouse gas (GHG) emissions.

It is important to highlight that a fraction of the influent organic matter is consumed by SRB, which meant it was not available for biogas production by methanogenic organisms. Specifically, 2 g of influent COD were consumed by SRB for each gram of sulfate (stoichiometrically).

Over-dimensioned equipment in the prototype plant prevented the direct measurement of electrical power consumption from being representative of the energy requirements of AnMBR technology. The power required by the equipment (pumps and blowers) was therefore calculated theoretically using the equations proposed by Judd and Judd [17] and Pretel et al. [26]. Adiabatic indexes, and blower and pump efficiencies were estimated based on standard values for these components.

Two sources of GHG emissions were considered: i) indirect CO_2 emissions related to the NED of the system ($CO_{2_{NED}}$) and ii) direct equivalent CO_2 emissions from dissolved methane in the effluent (CO_{2D-CH_4}). Both sources are considered as the main GHG contributors during the operation of the demo plant. It should be noted that, according to the IPCC2013 application guides, since they are included in a short-term carbon cycle, CO_2 emissions of biogenic origin produced during anaerobic digestion can be excluded from GHG calculations, as well as those associated with the subsequent combustion of biogas in a CHP unit. Three different values were calculated for CO_{2D-CH_4} and therefore for total CO_2 emissions: i) without dissolved methane recovery; ii) with 50 % of dissolved methane recovery and iii) with 70 % of dissolved methane recovery. Percentages of 50 % and 70 % were assumed based on the optimum economic and environmental results from previous studies, respectively [35].

Details on data calculations are provided as supplementary material.

3. Results and discussion

3.1. Filtration process performance

Fig. 1 gives the performance of the filtration process during the complete experimental period for the MT_A, MT_B and MT_C membrane tanks (average values can be seen in table S1 of the supplementary material). The black dashed bars indicate short maintenance stops (days 94 and 442) and gray dotted-dashed bars indicate membrane chemical cleanings (days 128 and 363). A conservative maximum TMP security value of 500 mbar was selected based on the supplier's information. Finally, the TSS concentration depicted in Fig. 1 corresponds to the reactor mixed liquor (i.e. MLSS), thus representing the TSS

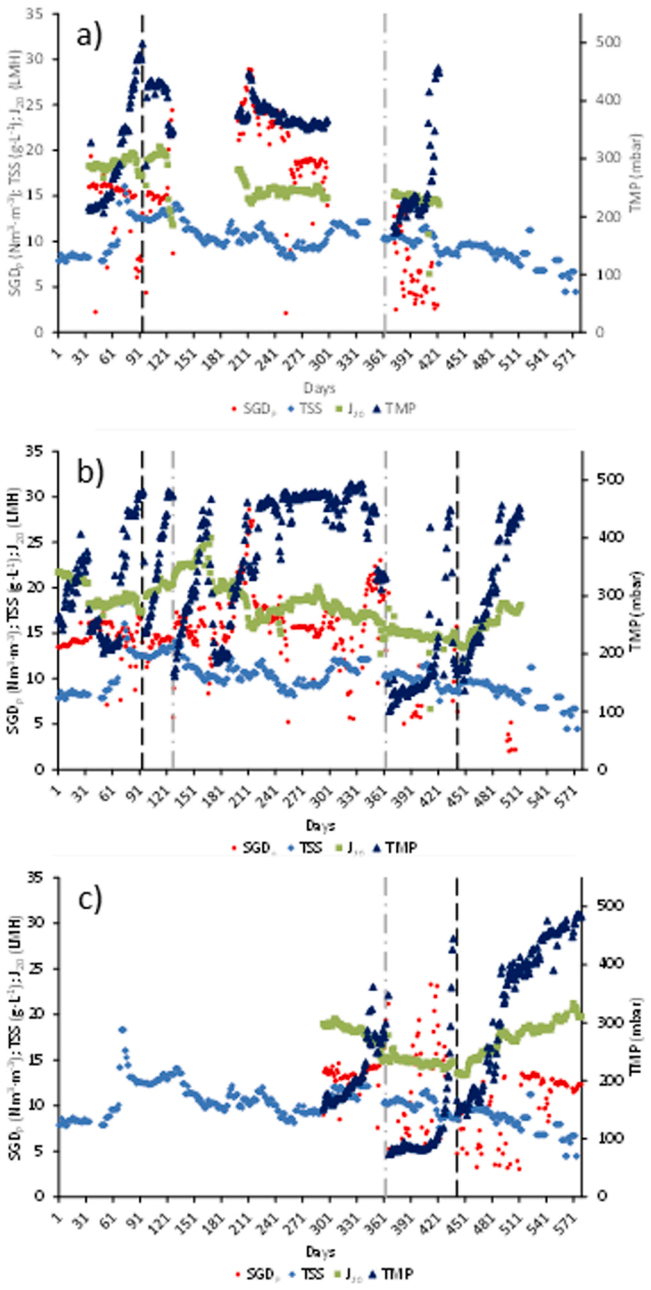

Fig. 1. Evolution of sparging gas demand per m^3 of permeate (SGD_P), gross 20°C-standardized transmembrane flux (J_{20}), transmembrane pressure during filtration stage (TMP) and total suspended solids (TSS) in a) MT_A; b) MT_B and c) MT_C. (Maintenance stop: black dashed line; Membrane chemical cleanings: gray dotted-dashed lines).

concentration of the mixed liquor entering the three MTs.

As can be seen in Fig. 1, J_{20} was maintained in similar values for all MTs: 14–20, 15–23 and 15–20 LMH for MT_A, MT_B, and MT_C, respectively. These J_{20} are somewhat higher than previous long-term AnMBR studies [15,24]. The J_{20} applied were also competitive against MBR for urban wastewater treatment. For instance, Xiao et al. [42] evaluated 19 large-scale Chinese MBRs and reported fluxes in the range of 15–25 LMH (19.6 LMH on average).

Regarding SGD_m, MT_A was operated between 0.1 and 0.4 $Nm^3 \cdot m^{-2} \cdot h^{-1}$; MT_B mostly at 0.3 $Nm^3 \cdot m^{-2} \cdot h^{-1}$, although higher (0.35–0.40 $Nm^3 \cdot m^{-2} \cdot h^{-1}$; days 130–200) and lower (0.1–0.2 $Nm^3 \cdot m^{-2} \cdot h^{-1}$; days 360–500) values were also evaluated; and MT_C at 0.25 $Nm^3 \cdot m^{-2} \cdot h^{-1}$ at days 294–360 and 510–580 and in the range of 0.1–0.3 $Nm^3 \cdot m^{-2} \cdot h^{-1}$ between days 360 and 510. The modifications in the applied SGD_m aimed to assess gas sparging intensity for fouling control.

In this operation, SGD_P varied between 7 and 23 $Nm^3 \cdot m^{-3}$ for MT_A and between 14 and 16 $Nm^3 \cdot m^{-3}$ for MT_B, with short periods above 20 $Nm^3 \cdot m^{-3}$ (e.g. days 200–216) and below 10 $Nm^3 \cdot m^{-3}$ (days 383–401). Fig. 1c gives the first period of MT_C, with SGD_P at 13–14 $Nm^3 \cdot m^{-3}$ (days 294–360), a second highly variable period between 5 and 22 $Nm^3 \cdot m^{-3}$ and a third period with SGD_P steady at around 12–13 $Nm^3 \cdot m^{-3}$.

Fig. 1 allows the comparison of the filtration performance of the three MTs, attending to the differences in their operation. Between days 31 and 91, MT_A and MT_B (see Fig. 1a and b) operated at similar J_{20} (16–20 LMH) and SGD_P (15–16 $Nm^3 \cdot m^{-3}$) and both tanks started from a close TMP, in the 210–220 mbar range. It can be observed that the behavior of both MTs was very similar, reaching in both cases the limit value of ≈ 500 mbar at the same time (day 91). It can also be observed a sharp increase in TSS on day 45, reaching a concentration of 15 $g \cdot L^{-1}$ around day 75, which coincides with the sharp TMP increase recorded in both tanks. Therefore, it can be concluded that the membranes were operated at supra-critical filtration conditions due to the combination of the J_{20}, SGD_P and TSS values within the experimental period.

After the maintenance stop conducted between days 91 and 94, both MT_A and MT_B partly reduced their TMP without applying any membrane chemical cleaning, thus the observed recovery was associated with reversible fouling that was removed as a result of prolonged air-assisted membrane scouring without filtration.

After restarting filtration, the behavior of both tanks differed. In the case of MT_A, there was an abrupt rise in TMP after only three days of operation, reaching a stable TMP around 420 mbar. From day 121, the J_{20} was reduced from 20 LMH to 12 LMH, and this caused a drop in the TMP from 420 to 330 mbar, which represents a reduction of 21 %. This TMP profile would indicate that reducing J_{20} turned the filtration process from supra-critical/critical (since TMP first raised and then could be maintained at 420 mbar) to sub-critical conditions. In MT_B, the filtration process caused a constant increase in TMP until reaching the maximum threshold value (i.e. 500 mbar) set for conducting a membrane chemical cleaning. On day 128, the membrane in MT_B was chemically cleaned, which reduced TMP to 161 mbar. A reduction of 43 % in membrane total resistance ($R_T^{\}$) when comparing the R_T achieved after the first maintenance stop on days 91–94 (i.e. 14.1 $LMH \cdot mbar^{-1}$) and the chemical cleaning on day 128 (i.e. 8.1 $LMH \cdot mbar^{-1}$) would indicate the amount of irreversible fouling accumulated on the MT_B membrane when the maintenance stop was conducted (between days 91 and 94). Eventually, filtration performance of MT_B between days 128 and 221 confirms that the combination of J_{20} above 20 LMH, SGD_P below 17 $Nm^3 \cdot m^{-3}$ and TSS above 10 $g \cdot L^{-1}$ led to significant fouling propensities, increasing TMP from 150 to 190–470 in 35–40 days.

Different profiles between MT_A and MT_B regarding J_{20}, SGD_P and TMP can be observed from day 200 and 295. Specifically, the reduction in J_{20} from 17.5 to 15–16 LMH applied to the MT_A managed to reduce the TMP from the maximum of 450 mbar to 360 mbar (day 245). Moreover, the reduction recorded in the TSS concentration from 11 to 9 $g \cdot L^{-1}$ also favored reducing the SGD_m from 0.37 to 0.29 $Nm^3 \cdot m^{-2} \cdot h^{-1}$ (corresponding to a SGD_P of 23 and 19 $Nm^3 \cdot m^{-3}$, respectively), resulting in a slight decrease in TMP, thus confirming that filtration was carried out under sub-critical conditions with this combination of J_{20}, SGD_m and TSS concentration. In this same period, MT_B was operated with a rising J_{20} from 15.5 LMH to 21 LMH and a SGD_m of 0.29 $Nm^3 \cdot m^{-2} \cdot h^{-1}$ (SGD_P of 19 $Nm^3 \cdot m^{-3}$) in average. These operating conditions resulted in a sharp TMP increase from 320 mbar to 460 mbar (day 225). Despite this increase, the reduction in TSS concentration to 10 $g \cdot L^{-1}$ allowed to offset the effect of increasing J_{20} on TMP thus managing to remain stable TMP values of around 470 mbar, which indicated that sub-critical filtration conditions were kept. It is also worth to highlight the drop in TMP that occurred between days 290 and 300 due to a decrease in J_{20} from 21 LMH to 16 LMH and the subsequent TMP increase observed when the TSS concentration increased from day 300. Thus, slight changes on J_{20} and/or SGD_m quickly allowed compensating the effect of TSS concentration on TMP, highlighting the potential of gas-assisted membrane scouring as physical fouling control strategy to keep sub-critical/critical filtration conditions thereby controlling membrane fouling propensity.

Between days 300 and 363, when a second membrane chemical cleaning was conducted, MT_B and MT_C were operated in parallel. Fig. 1b shows how MT_B experimented a TMP reduction due to increasing the SGD_m up to 0.35 $Nm^3 \cdot m^{-2} \cdot h^{-1}$ (corresponding to a SGD_P of 20 $Nm^3 \cdot m^{-3}$) between days 344 and 361. MT_C was operated at similar J_{20} values than the ones established in MT_B, although a constant SGD_m of 0.24 $Nm^3 \cdot m^{-2} \cdot h^{-1}$ (SGD_P of 13 $Nm^3 \cdot m^{-3}$) was established in MT_C. Thus, it can be concluded that, while it was possible to control TMP in MT_B by increasing gas sparging intensity, TMP in MT_C continuously increased between days 300 and 363. Therefore, MT_B operated at sub-critical filtration conditions (J_{20} of 15–18 LMH, SGD_P of 15–20 $Nm^3 \cdot m^{-3}$ and TSS of 12 $mg \cdot L^{-1}$) and MT_C at supra-critical filtration conditions (J_{20} of 15–18 LMH, SGD_P of 13–14 $Nm^3 \cdot m^{-3}$ and TSS of 12 $mg \cdot L^{-1}$).

On day 363, a chemical cleaning was conducted in the three MTs. In the case of MT_A, TMP turned out to similar values to the original ones (day 30). Thus, fouling was properly removed through chemical cleaning, revealing negligible levels or irremovable fouling on the membrane within the experimental period. In the case of MT_B, the R_T values achieved after this second chemical cleaning (i.e. 6.7 $LMH \cdot mbar^{-1}$) suggested that the first one (day 128) was not able to completely recovering irreversible fouling, i.e. around 1.4 $LMH \cdot mbar^{-1}$ of R_T was additionally removed compared to the results from the first chemical cleaning applied. In the case of MT_C, R_T was reduced to around 4.9 $LMH \cdot mbar^{-1}$, lower than the initial TMP on day 294 (i.e. 7.9 $LMH \cdot mbar^{-1}$), which would indicate the presence of previous fouling, since this membrane was kept submerged in the mixed liquor.

During days 361–445, the three MTs were operated in parallel. J_{20} between 14 and 15 LMH and low SGD_m (mostly 5–6 $Nm^3 \cdot m^{-2} \cdot h^{-1}$) were established for MT_A and TM_B. MT_C was operated at J_{20} of 15 LMH and higher but fluctuating SGD_P (5–21 $Nm^3 \cdot m^{-3}$). Around day 400, a sharp increase in TMP up to 460–480 mbar was observed in MT_A and MT_B driven by the low agitation, while MT_C could sustain filtration at low TMP for a few days longer (until day 420) since it was operated with higher SGD_P.

Finally, a maintenance stop was conducted on day 443. After this stop, R_T did not reach the value obtained after the previous chemical cleaning, thus some irreversible fouling (around 5 $LMH \cdot mbar^{-1}$ equivalent) may be developed from day 363–443 During this period, MT_B and MT_C were operated at similar J_{20} and SGD_m levels. Indeed, both tanks resulted in similar TMP behaviors. From day 505, only the MT_C was operated and its SGD_m was increased to 0.24 $Nm^3 \cdot m^{-2} \cdot h^{-1}$ (corresponding to an SGD_P of 12.5 $Nm^3 \cdot m^{-3}$). This increase resulted in a significant reduction in TMP growth rate and therefore in fouling rate (i.e. from 4.1 $mbar \cdot d^{-1}$ to 1.4 $mbar \cdot d^{-1}$).

Therefore, Fig. 1 shows the complex interaction between J_{20}, SGD_m (as shown by SGD_P), TSS in the reactor, TMP and the evolution of fouling. Operation at high J_{20} with low fouling propensities can be

achieved with high SGD_m and low mixed liquor TSS concentrations. These results are in line with those obtained elsewhere by Mei et al. [23].

The results show that the system was able to conduct filtration at a moderate-high J_{20} (15–20 LMH) with competitive SGD_m (at an SGD_P of 10–20 $Nm^3 \cdot m^{-3}$) and moderate TSS (8–13 $g \cdot L^{-1}$), although shifts between supra-critical and subcritical filtration were seen to occur with small changes in the operating conditions. Operating at sub-critical filtration conditions (recommended to avoid quick TMP increase) was possible with TSS concentrations below 10 $g \cdot L^{-1}$, maximum J_{20} of 16 LMH and SGD_m of 0.3 $Nm^3 \cdot m^{-2} \cdot h^{-1}$ (corresponding to 15 $Nm^3 \cdot m^{-3}$). Fig. 1 also shows that fouling control can be achieved even at high TMP (e.g. between days 210 and 300 in MT_A (380–400 mbar) or between days 210 and 335 in MT_B (470–500 mbar). During these periods, the TMP presented a plateau profile, which indicated negligible fouling propensity. In this sense, the rapid response of TMP to changes in J_{20} and/or SGDm contributes to facilitate fouling control. However, operating at high TMP would imply increasing energy requirement for permeate pumping and increasing dissolved methane concentration. Therefore, to avoid these drawbacks operation at high TMP is not advisable.

As filtration performance comparison, [18] operated a pilot-scale AnMBR to treat municipal wastewater at ambient temperature (25 °C) and reported significantly lower transmembrane fluxes of approx. 3 and 4.5 LMH for HRT of 48 and 24 h, respectively, despite experiments at HRT of 24 h were conducted with lower mixed liquor suspended solids, in the 6.7–10.2 $g \cdot L^{-1}$ range (mixed liquor suspended solids at HRT of 48 h were not included in the study). Shin & Bae [37] described the performance of different pilot scale AnMBR treating domestic wastewater. These authors found that the most common transmembrane fluxes were in the 6–14 LMH range, while applied SGD_m varied mostly between 0.15 and 0.31 $Nm^3 \cdot m^{-2} \cdot h^{-1}$. Lee & Liao, [11] considered 10 LMH as typical design parameter for transmembrane flux.

Finally, it should be noted that the demo plant achieved a successful long-term operation without chemical cleaning requirements, the longest operation period being 233 days of MT_B (days 128–363), although the results indicate that longer operating periods could be achieved. No irrecoverable fouling was detected during the study since chemical cleaning returned the TMP to the initial values or even lower.

3.2. Energy assessment

Evolution of biogas production, its methane content expressed in percentage of CH_4, and removed COD (% COD_{rem}) can be found in supplementary materials. Moreover, details on the evolution of biogas production process in this demo plant during this operational period can be found in Robles et al. [29], where it could be concluded that temperature, HRT, SRT and influent $COD \cdot SO_2^{-4}$-S ratio showed crucial influence in biogas production.

As already mentioned in Section 2.2, organic load and temperature varied according to economic activities and ambient conditions, respectively. Methane production is therefore highly influenced by these factors. Periods with high temperature and high OL-MA showed higher biogas productions. Conversely, low OL-MA and low temperature led to reduced biogas production. With regards to methane content in the biogas, it remained mostly above 70 % (75 ± 3 % on average). Finally, AnMBR reached a significant COD removal efficiency (89 ± 5 % on average) (further details can be found in Fig. S3 of supplementary materials).

Fig. 2 shows the evolution of EC, TER and NED. The gaps in the figures are due to maintenance stops and failures in the online equipment required for calculations.

Fig. 2a shows an initial period between days 1–30 with high energy consumption for reactor mixing (around 0.11 $kWh \cdot m^{-1}$). On day 31, mixing was reduced to 0.04–0.08 $kWh \cdot m^{-3}$ until day 500, without affecting reactor performance. EC related to membrane scouring also varied according to the applied SGD_m and number of membrane tanks in

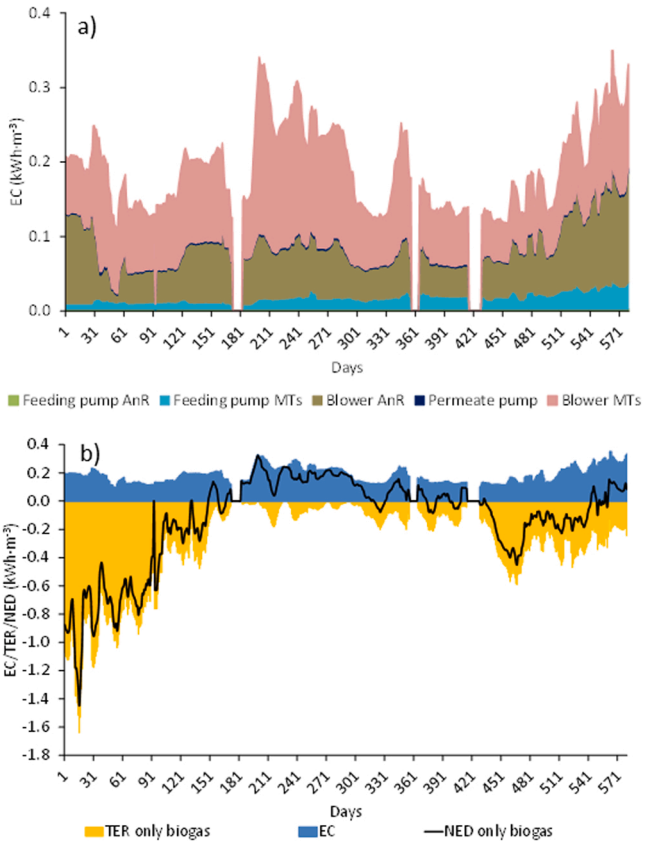

Fig. 2. Results of (a) allocation of energy consumption (EC) per equipment and (b) total energy consumption (EC), total energy recovery (TER) and net energy demand (NED) considering only the energy recovered from biogas (only biogas).

operation. Between days 1–30, only MT_B was in operation at an SGD_m of 0.3 $Nm^3 \cdot m^{-2} \cdot h^{-1}$. On day 35, MT_A started operating jointly with MT_B, leading to an increased need for sparging and higher energy consumption (1.2–1.3 $kWh \cdot m^{-3}$). MT_A and MT_B were also operated in parallel between days 194–299, when energy consumption reached the highest value (1.5–2.0 $kWh \cdot m^{-3}$), which was associated with higher applied SGD_m in MT_A (0.36–0.43 $Nm^3 \cdot m^2 \cdot h^1$). From day 300, MT_A was stopped, SGD_m in MT_B was reduced to 0.20 $Nm^3 \cdot m^2 \cdot h^1$ and MT_C started with an applied SGD_m of 0.24 $Nm^3 \cdot m^2 \cdot h^1$. Energy consumption for membrane scouring was thus reduced to 0.5–0.6 $kWh \cdot m^3$. On days 330–355, SGD_m in MT_B was set to 0.35 $Nm^3 \cdot m^2 \cdot h^1$, which led to higher energy consumption for membrane scouring. The period between days 365–500 was characterized by lower applied SGD_m (and thus SGD_P) than previously, which allowed moderate-low energy consumption despite MT_B and MT_C being operated in parallel, and MT_A was jointly operated between days 373–420. The EC associated with membrane tank feeding mostly remained below 0.02 $kWh \cdot m^{-3}$ while the energy requirement for the reactor feeding pump was negligible. After day 500, HRT was set to 70 h, so that the treatment flow was reduced, leading to higher specific energy consumption in $kWh \cdot m^{-3}$.

Fig. 2b gives the total EC, TER and NED. The TER in Fig. 2b was based on energy recovered from the biogas stream only (0 % of dissolved methane recovery). This recovered energy allowed the plant to perform as a net energy producer for over 50 % of the study period (negative values in NED). As can be seen in Fig. 2b, methane production and therefore energy recovery was boosted by a high OL-MA and temperature (see Fig. S2 in supplementary materials). In this regard, TER followed the same trend as the temperature from day 1–160, with a high energy production at 28 °C (days 1–60), which dropped steadily as the temperature dropped to 14 °C (day 160). Days 440–580 also showed

high TER values, when energy production increased when the temperature remained above 26 °C (days 400–450) and by the increase in OL-MA (days 450–490). On the other hand, days 160–440 resulted in reduced TER since this period was characterized by a relatively low temperature and OL-MA.

Table 2 gives the average results for the entire study period and shows that the main contributions to EC were associated with the blower requirements for membrane scouring (55.2 %), followed by reactor mixing (34.4 %). Conversely, membrane tanks' feeding pump, filtration pumps, and reactor feeding pump had comparatively very low energy consumption (7.8 %, 1.6 % and 1.0 %, respectively). The contribution of the degassing membrane blowers was negligible (<0.02 %). Overall, average EC accounts for 0.192 ± 0.070 kWh·m^{-3} while average TER (0 % methane recovery) was 0.361 ± 0.271 kWh·m^{-3}. Dissolved methane produced more energy than that used in its recovery, although its contribution to TER was relatively low (between 0.02 kWh·m^{-3} and 0.04 kWh·m^{-3} for dissolved methane recovery ratios of 50% and 70 %, respectively). However, this recovery definitively reduced GHG emissions, as will be explained in the following section.

These results can be compared with other studies dealing with AnMBR for wastewater treatment. Rong et al. [4] evaluated the energy balance of an AnMBR at pilot scale and a projected scaled-up facility of 10000 m^3·d^{-1}. Influent COD was 331–414 mg·L^{-1} and temperature ranged between 15 and 25 °C. These authors obtained a net electricity demand in the 0.09–0.10 kWh·m^{-3} range, with gas sparging accounting for 52.46–74.60 % and reactor mixing for 4.08–6.13 %. More specifically, Hu et al. [14] reported energy consumptions for gas sparging between 0.25 and 3.4 kWh·m^{-3}, accounting for approx. 70 % of total energy consumption, which are between 2 and 32 times the average energy consumption obtained in this study (0.106 ± 0.047 kWh·m^{-3}). Concerning degassing membranes, lower energy consumptions were achieved (between $2.3{\cdot}10^{-5}$ ± $3.4{\cdot}10^{-6}$ and $4.3{\cdot}10^{-5}$ ± $6.3{\cdot}10^{-6}$ kWh·m^{-3}, see Table 2) compared to the one reported by Velasco et al. [40], i.e. 0.01 kWh·m^{-3} for 90 % of dissolve methane recovery.

Moreover, Krzeminski et al. [19] reported 0.3–0.6 kWh·m^{-3} for CAS and 0.6–2.3 kWh·m^{-3} for MBR, including nutrient removal. In this sense, Fraia et al. [8] reported energy consumption for nitrogen removal up to 6.08 kWh per kg of influent total nitrogen (kWh·TN$_{in}$) in wastewater treatment facilities with high nitrogen removal efficiency (> 89.2 %), while energy consumption associated to phosphorus removal was considered negligible. Hence, assuming the nitrogen load of the AnMBR influent (see Table 1) the energy demand for nitrogen removal in an aerobic/anoxic process would be of approx. 0.29 kWh·m^{-3}, according to this literature value. Hence, extracting this value to the above-mentioned ranges for CAS and MBR energy demand, the energy consumption related to COD removal in CAS and MBR technology would be between 0.01 and 0.31 and 0.31–1.99 kWh·m^{-3}, respectively. These estimated range of energy requirements would be still higher than the average NED reported in this study when dissolved methane recovery is not conducted (−0.169 ± 0.341 kWh·m^{-3}; see Table 2).

Table 2
Energy consumption (EC), total energy recovery (TER) and net energy demand (NED) for 0 %, 50 % and 70 % of dissolved methane recovery (D-CH4).

	D-CH$_4$ Recovery fraction		
kWh·m^{-3}	*0%*	*50%*	*70%*
EC blower DM	-	$2.3{\cdot}10^{-5}$ ± $3.4{\cdot}10^{-6}$	$4.3{\cdot}10^{-5}$ ± $6.3{\cdot}10^{-6}$
EC blower AnR	0.066 ± 0.030		
EC blower MT	0.106 ± 0.047		
EC AnR feeding pump	0.002 ± 0.000		
EC MT feeding pump	0.015 ± 0.007		
EC permeate pump	0.003 ± 0.001		
Total EC	0.192 ± 0.070		
TER	0.361 ± 0.271	0.382 ± 0.306	0.397 ± 0.377
NED	***-0.169 ± 0.341***	***-0.190 ± 0.376***	***-0.205 ± 0.447***

These results emphasize the importance of optimizing the parameters governing the reactor mixing requirements and filtration, especially with regard to SGD$_m$. Increasing sludge recycling would reduce TSS concentration in the MTs and help to reduce SGD$_m$ necessities. Since the MT feeding pump represents only 8 % of EC and membrane scouring accounts for 55 %, this strategy could improve the AnMBR energy performance through a slight increase in the consumption of the sludge pump, which would be compensated by a larger reduction of consumption for membrane scouring. This sludge circulation could also be used to promote reactor mixing and would reduce its energy consumption (34 %).

It should be noted that the significant sulfate content in the influent favors SRB growth, so that improved AnMBR energy performance could be expected when treating low-sulfate wastewater [29].

3.3. GHG emissions

Fig. 3 shows the equivalent CO_2 emissions associated with dissolved CH_4 (D-CH_4) when no recovery is considered (gray area) and net GHG emissions (including D-CH_4 and those associated with EC) considering 0 %, 50 % and 70 % of dissolved methane recovery (orange, blue and green lines respectively).

When no methane recovery was considered, the contribution of D-CH_4 to total emissions accounted for 0.5–0.6 kgCO_{2eq}·m^{-3} during almost the entire period of plant operation. The periods in which the orange line is lower than the corresponding gray bar indicate net energy production (e.g. days 1–130, see Fig. 2a). On these days, savings in indirect CO_2 emissions related to energy production generated a *GHG credit* which reduced the total carbon footprint. This effect was also found to a lesser extent during days 430–480. Conversely, the orange line over the gray area indicates emissions related to net EC, which is added to those of dissolved methane release (days 210–340).

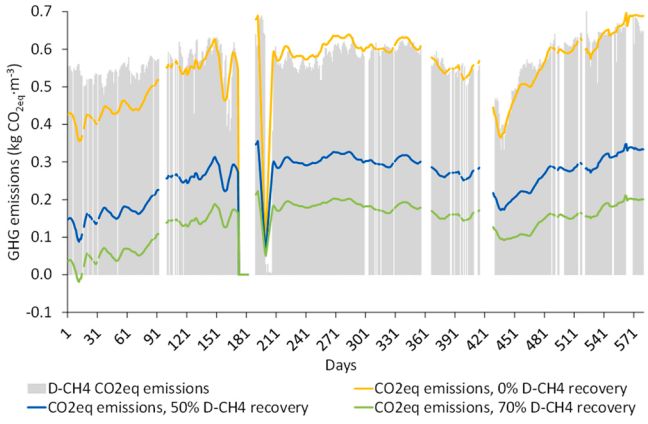

Fig. 3. Evolution of GHG emissions in the operating phase of the demonstration plant: direct CO_2 equivalent emissions of dissolved methane (gray bars), and CO_2 equivalent emissions when considering NED and dissolved methane recovery of 0 % (orange), 50 % (blue) and 70 % (green). (For interpretation of the references to color in this figure legend, the reader is referred to the web version of this article.)

Net GHG emissions with 0 % of methane recovery (orange line) showed values around 0.4 $kgCO_{2eq}·m^{-3}$, when high volumes of biogas were produced and energy recovery was significantly high (days 1–130), whereas the value oscillates around 0.6 $kgCO_{2eq}·m^{-3}$ when low biogas production was obtained. According to Sanchis-Perucho et al. [35], the economic optimum for dissolved methane recovery would be 50 % and the environmental optimum 70 % approx. The results obtained with 50 % and 70 % of dissolved methane recovery (blue and green lines, respectively) show the importance of this process for the improvement of the overall AnMBR environmental performance by reducing CH_4 emissions. For instance, recovering 50 % of the methane would reduce the equivalent CO_2 emissions to 0.1–0.3 $kgCO_{2eq}·m^{-3}$. Operating with 70 % methane recovery kept the emissions below 0.2 $kgCO_{2eq}·m^{-3}$ during the entire study period. By way of comparison, Rodriguez-Garcia et al. [33] estimated emissions of around 0.3 $kgCO_{2eq}·m^{-3}$ for CAS facilities with organic matter and nutrient removal discharging in sensitive areas, while Chen [6] estimated small-scale MBR (351 $m^3·d^{-1}$ treatment capacity) emissions to be around 0.7 $kgCO_2·m^{-3}$.

The GHG emissions associated with D-CH_4 appear as the main contributor to this environmental impact (between 83.8 % and 95.7 %). Since the other contributors are derived from power consumption, the higher use of renewable energies in the energy mix will raise these percentages even further. The improvement of AnMBR will necessarily involve further research in systems of dissolved methane recovery to offset CO_2 emissions. In this regard, AnMBR combined with degassing membranes represents a promising combination, as it merges greater energy recovery with the possibility of reducing GHG emissions [12].

Increasing energy recovery would also help to widen the applicability of AnMBR technology, for example co-digestion of wastewater with other substrates (organic fraction of food waste, food industry wastewater, etc.) has been successfully explored [26]. Biogas upgrading is another strategy that takes advantage of methane; this option has recently received great attention in the UE (e.g. REPowerEU Plan) and promising environmental and economic results have been obtained [3].

Finally, it is important to highlight the additional benefits that recovering nutrients would entail, since N and P production from traditional sources require high power consumption and GHG emissions. McCarty et al. [22] reported 19.3 kWh per kg N and 2.11 kWh per kg P. According to these values, considering the average N and P content in the effluent (45.7 ± 10.4 mg $N·L^{-1}$ and 7.8 ± 2.0 mg $P·L^{-1}$, data not shown) and a GHG emission factor for Spanish energy mix generation of 0.14 kg CO_2.kWh [28], fertigation would allow savings of 0.126 kg $CO_{2eq}·m^{-3}$, which would help the combination of AnMBR+fertigation to achieve carbon neutrality if 70 % of the dissolved methane was recovered.

The results of this study suggest that AnMBR shows promise as a potential technology for reducing the energy dependence and overall environmental impacts of wastewater treatment. The combination of anaerobic treatments and membrane technology in AnMBR paves the way for turning wastewater into a source of resources. Energy, nutrients and reclaimed water could be supplied by the continuously generated sewage, while this approach complies with the fundamental principles of the CE and is fully aligned with the Sustainable Development Goals.

4. Conclusions

An industrial AnMBR wastewater treatment prototype was successfully operated for 580 days. Fouling propensity remained low and long-term operations were achieved, with a maximum continuous operation of 233 days without applying membrane chemical cleaning. The UF modules were able to operate at a high J_{20} in the range of 15–20 LMH and a competitive SGD_m of between 0.1 and 0.4 $Nm^3·m^{-2}·h^{-1}$ (which corresponded to a SGD_P of 10–20 $Nm^3·m^{-3}$). TMP showed a quick response to changes in J_{20} and SGD_m, which facilitated fouling control. Moreover, operation with TSS concentrations below 10 $g·L^{-1}$, J_{20} of 16 LMH and SGD_m of 0.3 $Nm^3·m^{-2}·h^{-1}$ (corresponding to 15 $Nm^3·m^{-3}$) would further lengthen the filtration periods between chemical cleanings.

With regards to energy assessment, the average EC was estimated at 0.192 ± 0.070 $kWh·m^{-3}$, with most of the power consumed by membrane scouring (55 %) and reactor mixing (34 %). The valorization of organic matter provided an average TER of 0.361 ± 0.271, 0.382 ± 0.306 and 0.397 ± 0.377 $kWh·m^{-3}$ with 0 %, 50 % and 70 % recovery of dissolved methane, respectively, obtaining a NED of − 0.169 ± 0.341, − 0.190 ± 0.376 and − 0.205 ± 0.447 $kWh·m^{-3}$, respectively. The increase in energy production associated with the recovery of dissolved methane is therefore low, but higher than the energy consumption of degassing membranes. Finally, dissolved methane recovery appears as the key challenge to be overcome for achieving low GHG emissions with AnMBR. In this study, recoveries of 50 % and 70 % reduced emissions from 0.5 to 0.6–0.1–0.3 and below 0.2 $kgCO_2·m^{-3}$, respectively.

Overall, the AnMBR demo plant showed a suitable filtration performance, significant energy productions and low CO_2 emissions when recovering dissolved methane. These results indicate that AnMBR combined with degassing membranes represents a robust alternative to the conventional wastewater treatment.

CRediT authorship contribution statement

A. Jiménez-Benítez: Writing – original draft, Investigation, Methodology, Formal analysis, Writing – review & editing. **A. Ruiz-Martínez:** Investigation, Methodology, Resources, Writing – review & editing. **Á. Robles:** Investigation, Methodology, Formal analysis, Validation, Writing – review & editing. **J. Serralta:** Resources, Investigation, Validation, Writing – review & editing. **J. Ribes:** Resources, Investigation, Management and coordination responsibility for the research activity planning and execution, Validation, Writing – review & editing. **F. Rogalla:** Investigation, Methodology, Resources. **A. Seco:** Definition, Methodology, Formal analysis, Investigation, Validation, Writing – review & editing, Supervision, Management and coordination responsibility for the research activity planning and execution. **J. Ferrer:** Methodology, Formal analysis, Investigation, Validation, Writing – review & editing, Supervision, Management and coordination responsibility for the research activity planning and execution.

Declaration of Competing Interest

The authors declare that they have no known competing financial interests or personal relationships that could have appeared to influence the work reported in this paper.

Data availability

Data will be made available on request.

Acknowledgement

The authors are grateful to the European Commission for the co-financing of the LIFE MEMORY Project (LIFE13 ENV/ES/ 001353) and the staff of Aguas de Alcázar for their collaboration.

Appendix A. Supporting information

Supplementary data associated with this article can be found in the online version at doi:10.1016/j.jece.2023.109454.

References

[1] Robles, Ángel, Serralta, J., Martí, N., Ferrer, J., Seco, A. , (2021). Anaerobic membrane bioreactors for resource recovery from municipal wastewater: a comprehensive review of recent advances, Environ. Sci.: Water Res. Technol., 7 (11), 1944–1965. https://doi.org/10.1039/d1ew00217a.

[2] APHA, (2005). Standard Methods for the Examination of Water and Wastewater, twenty first ed., American Public Health Association.

[3] F. Ardolino, G.F. Cardamone, F. Parrillo, U. Arena, Biogas-to-biomethane upgrading: a comparative review and assessment in a life cycle perspective, Renew. Sustain. Energy Rev. 139 (2021), 110588, https://doi.org/10.1016/j.rser.2020.110588.

[4] C. Rong, T. Wang, Z. Luo, Y. Hu, Z. Kong, Y. Qin, Y. Li , Seasonal and Annual Energy Efficiency of Mainstream Anaerobic Membrane Bioreactor (AnMBR) in Temperate Climates : Assessment in Onsite Pilot Plant and Estimation in Scaled-up Plant (2022) 360(June).

[5] Chen, R., Chang, S., Hong, Y., & Wu, P. , (2015). Brewery wastewater treatment by anaerobic membrane bioreactor, in: Proceedings of the Annual Conference - Canadian Society for Civil Engineering, 1_2015, 390–399.

[6] Y.C. Chen, Estimation of greenhouse gas emissions from a wastewater treatment plant using membrane bioreactor technology, Water Environ. Res. 91 (2) (2019) 111–118, https://doi.org/10.1002/wer.1004.

[7] F. Durán, Á. Robles, J.B. Giménez, J. Ferrer, J. Ribes, J. Serralta, Modeling the anaerobic treatment of sulfate-rich urban wastewater: application to AnMBR technology, Water Res. (2020) *184*, https://doi.org/10.1016/j.watres.2020.116133.

[8] S.Di Fraia, N. Massarotti, L. Vanoli, A novel energy assessment of urban wastewater treatment plants, Energy Convers. Manag. 163 (2018) 304–313, https://doi.org/10.1016/j.enconman.2018.02.058.

[9] Giménez, J.B., Martí, N., Ferrer, J., Seco, A. , (2012). Methane recovery efficiency in a submerged anaerobic membrane bioreactor (SAnMBR) treating sulphate-rich urban wastewater: evaluation of methane losses with the effluent, Bioresour. Technol., 118, 67–72. https://doi.org/10.1016/j.biortech.2012.05.019.

[10] J.S. Guest, S.J. Skerlos, J.L. Barnard, M.B. Beck, G.T. Daigger, H. Hilger, S. J. Jackson, K. Karvazy, L. Kelly, L. Macpherson, J.R. Mihelcic, A. Pramanik, L. Raskin, M.C.M. Van Loosdrecht, D. Yeh, N.G. Love, A new planning and design paradigm to achieve sustainable resource recovery from wastewater, Environ. Sci. Technol. 43 (16) (2009) 6126–6130, https://doi.org/10.1021/es9010515.

[11] H. Lee, B. Liao, Anaerobic Membrane Bioreactors for Wastewater Treatment: Challenges and Opportunities (2021). doi: 10.1002/wer.1475.

[12] M. Henares, M. Izquierdo, P. Marzal, V. Martínez-Soria, Demethanization of aqueous anaerobic effluents using a polydimethylsiloxane membrane module: mass transfer, fouling and energy analysis, Sep. Purif. Technol. 186 (2017) 10–19, https://doi.org/10.1016/j.seppur.2017.05.035.

[13] D. Hu, T. Xiao, Z. Chen, H. Wang, J. Xu, X. Li, H. Su, Y. Zhang, Effect of the high cross flow velocity on performance of a pilot-scale anaerobic membrane bioreactor for treating antibiotic solvent wastewater, Bioresour. Technol. 243 (2017) 47–56, https://doi.org/10.1016/j.biortech.2017.06.030.

[14] Y. Hu, X. Cai, Y. Xue, R. Du, J. Ji, R. Chen, D. Sano, Y.-Y. Li, Recent developments of anaerobic membrane bioreactors for municipal wastewater treatment and bioenergy recovery: Focusing on novel configurations and energy balance analysis, J. Clean. Prod. 356 (2022), 131856, https://doi.org/10.1016/j.jclepro.2022.131856.

[15] J. Ji, S. Sakuma, J. Ni, Y. Chen, Y. Hu, A. Ohtsu, R. Chen, H. Cheng, Y. Qin, T. Hojo, K. Kubota, Y.Y. Li, Application of two anaerobic membrane bioreactors with different pore size membranes for municipal wastewater treatment, Sci. Total Environ. 745 (2020), 140903, https://doi.org/10.1016/j.scitotenv.2020.140903.

[16] Jiménez-Benítez, A., Ferrer, J., Rogalla, F., Vázquez, J.R., Seco, A., Robles, Á. , (2020). 12 - Energy and environmental impact of an anaerobic membrane bioreactor (AnMBR) demonstration plant treating urban wastewater, in: G. Mannina, A. Pandey, C. Larroche, H. Y. Ng, H. H. B. T. Ngo, (Eds.), Current Developments in Biotechnology and Bioengineering, Elsevier, 289–310. https://doi.org/https://doi.org/10.1016/B978–0-12–819854-4.00012–5.

[17] Judd, S., Judd, C. , (2006). Simon Judd, C. Judd, (Eds.), The MBR Book: Principles and Applications of Membrane Bioreactors for Water and Wastewater Treatment, Elsevier Science. https://doi.org/https://doi.org/10.1016/B978–1-85617–481-7.X5000–4.

[18] Z. Kong, J. Wu, C. Rong, T. Wang, L. Li, Z. Luo, J. Ji, Large pilot-scale submerged anaerobic membrane bioreactor for the treatment of municipal wastewater and biogas production at 25 ∘ C, Bioresour. Technol. 319 (2021), 124123, https://doi.org/10.1016/j.biortech.2020.124123.

[19] P. Krzeminski, L. Leverette, S. Malamis, E. Katsou, Membrane bioreactors – a review on recent developments in energy reduction, fouling control, novel configurations, LCA and market prospects, J. Membr. Sci. 527 (2017) 207–227, https://doi.org/10.1016/j.memsci.2016.12.010.

[20] Lazarova, V., Choo, K.-H., Cornel, P. , (2012). Water-Energy Interactions in Water Reuse, IWA Publishing. https://doi.org/10.2166/9781780400662.

[21] H.J. Lin, K. Xie, B. Mahendran, D.M. Bagley, K.T. Leung, S.N. Liss, B.Q. Liao, Sludge properties and their effects on membrane fouling in submerged anaerobic membrane bioreactors (SAnMBRs, Water Res. 43 (15) (2009) 3827–3837, https://doi.org/10.1016/j.watres.2009.05.025.

[22] P.L. McCarty, J. Bae, J. Kim, Domestic wastewater treatment as a net energy producer–can this be achieved, Environ. Sci. Technol. 45 (17) (2011) 7100–7106, https://doi.org/10.1021/es2014264.

[23] X. Mei, Z. Wang, Y. Miao, Z. Wu, Recover energy from domestic wastewater using anaerobic membrane bioreactor: operating parameters optimization and energy balance analysis, Energy 98 (2016) 146–154, https://doi.org/10.1016/j.energy.2016.01.011.

[24] M. Peña, T. do Nascimento, J. Gouveia, J. Escudero, A. Gómez, A. Letona, J. Arrieta, F. Fdz-Polanco, Anaerobic submerged membrane bioreactor (AnSMBR) treating municipal wastewater at ambient temperature: operation and potential use for agricultural irrigation, Bioresour. Technol. (2019), https://doi.org/10.1016/j.biortech.2019.03.019.

[25] R. Pretel, A. Robles, M.V. Ruano, A. Seco, J. Ferrer, Environmental impact of submerged anaerobic MBR (SAnMBR) technology used to treat urban wastewater at different temperatures, Bioresour. Technol. 149 (2013) 532–540, https://doi.org/10.1016/J.BIORTECH.2013.09.060.

[26] R. Pretel, A. Robles, M.V. Ruano, A. Seco, J. Ferrer, A plant-wide energy model for wastewater treatment plants: application to anaerobic membrane bioreactor technology, Environ. Technol. 37 (18) (2016) 2298–2315, https://doi.org/10.1080/09593330.2016.1148903.

[27] R.E., Moosbrugger, M.C. Wentzel, G.A. E., (1992). Simple Titration Procedures to Determine H2 CO3 " Alkalinity and Short-chain Fatty Acids in Aqueous Solutions.

[28] REE, (n.d.). Red eléctrica de España. https://www.ree.es/es/datos/generacion/no-renovables-detalle-emisiones-CO2. (Accessed 14 March 2022).

[29] Á. Robles, A. Jiménez-Benítez, J.B. Giménez, F. Durán, J. Ribes, J. Serralta, F. Rogalla, A. Seco, A semi-industrial scale AnMBR for municipal wastewater treatment at ambient temperature, Perform. Biol. Process. (2022) *215*, https://doi.org/10.1016/j.watres.2022.118249.

[30] Ángel Robles, F. Durán, M.V. Ruano, J. Ribes, A. Rosado, A. Seco, J. Ferrer, Instrumentation, control, and automation for submerged anaerobic membrane bioreactors, Environ. Technol. 36 (14) (2015) 1795–1806, https://doi.org/10.1080/09593330.2015.1012180.

[31] Ángel Robles, F. Durán, J. Bautista, E. Jiménez, J. Ribes, J. Serralta, A. Seco, J. Ferrer, F. Rogalla, Anaerobic membrane bioreactors (AnMBR) treating urban wastewater in mild climates, Bioresour. Technol. 314 (July) (2020), 123763, https://doi.org/10.1016/j.biortech.2020.123763.

[32] A. Rodriguez-Caballero, I. Aymerich, R. Marques, M. Poch, M. Pijuan, Minimizing N2O emissions and carbon footprint on a full-scale activated sludge sequencing batch reactor, Water Res. 71 (2015) 1–10, https://doi.org/10.1016/J.WATRES.2014.12.032.

[33] G. Rodriguez-Garcia, M. Molinos-Senante, A. Hospido, F. Hernández-Sancho, M. T. Moreira, G. Feijoo, Environmental and economic profile of six typologies of wastewater treatment plants, Water Res. 45 (18) (2011) 5997–6010, https://doi.org/10.1016/j.watres.2011.08.053.

[34] S. Solomon, D. Qin, M. Manning, Z. Chen, M. Marquis, K.B. Averyt, M. Tignor, H.L. Miller, IPCC, 2007: Climate Change 2007: The Physical Science Basis. Contribution of Working Group I to the Fourth Assessment Report of the Intergovernmental Panel on Climate Change, (2007). doi: 10.1256/wea.58.04.

[35] P. Sanchis-Perucho, A. Robles, F. Durán, J. Ferrer, A. Seco, PDMS membranes for feasible recovery of dissolved methane from AnMBR effluents, J. Membr. Sci. 604 (2020), 118070, https://doi.org/10.1016/j.memsci.2020.118070.

[36] Pau Sanchis-Perucho, Á. Robles, F. Durán, F. Rogalla, J. Ferrer, A. Seco, Widening the applicability of AnMBR for urban wastewater treatment through PDMS membranes for dissolved methane capture: effect of temperature and hydrodynamics, J. Environ. Manag. 287 (February) (2021), 112344, https://doi.org/10.1016/j.jenvman.2021.112344.

[37] C. Shin, J. Bae, Current status of the pilot-scale anaerobic membrane bioreactor treatments of domestic wastewaters: a critical review, Bioresour. Technol. 247 (2018) 1038–1046, https://doi.org/10.1016/j.biortech.2017.09.002.

[38] A.L. Smith, L.B. Stadler, L. Cao, N.G. Love, L. Raskin, S.J. Skerlos, Navigating wastewater energy recovery strategies: a life cycle comparison of anaerobic membrane bioreactor and conventional treatment systems with anaerobic digestion, Environ. Sci. Technol. 48 (10) (2014), https://doi.org/10.1021/es5006169.

[39] P. Velasco, V. Jegatheesan, M. Othman, Recovery of dissolved methane from anaerobic membrane bioreactor using degassing membrane contactors, Front. Environ. Sci. 6 (2018) 151, https://doi.org/10.3389/fenvs.2018.00151.

[40] P. Velasco, V. Jegatheesan, K. Thangavadivel, A focused review on membrane contactors for the recovery of dissolved methane from anaerobic membrane bioreactor (AnMBR) effluents, Chemosphere 278 (2021), 130448, https://doi.org/10.1016/j.chemosphere.2021.130448.

[41] S. Vinardell, J. Dosta, J. Mata-Alvarez, S. Astals, Unravelling the economics behind mainstream anaerobic membrane bioreactor application under different plant layouts, Bioresour. Technol. 319 (2021), 124170, https://doi.org/10.1016/j.biortech.2020.124170.

[42] K. Xiao, S. Liang, X. Wang, C. Chen, X. Huang, Current state and challenges of full-scale membrane bioreactor applications: a critical review, Bioresour. Technol. 271 (2019) 473–481, https://doi.org/10.1016/J.BIORTECH.2018.09.061.